# **ARTICLES**

## Atomistic Simulations of Corrosion Inhibitors Adsorbed on Calcite Surfaces I. Force field **Parameters for Calcite**

## Sungu Hwang,† Mario Blanco, and William A. Goddard III\*

Materials and Process Simulation Center, Beckman Institute (139-74), Division of Chemistry and Chemical Engineering, California Institute of Technology, Pasadena, California 91125

Received: February 14, 2001; In Final Form: July 23, 2001

We report a new force field for calcite suitable to study scale formation and squeeze treatments for oil field applications. The force field reproduces the cell parameters, density, and the compressibility of the calcite crystal as well as the enthalpy of immersion of various solvents. Surface energetics for the various surfaces of interest are predicted.

#### 1. Introduction

Corrosion inhibitors for oil pipelines are in general use in the petroleum industry. We recently reported the self-assembled monolayer mechanism for corrosion inhibition of iron by imidazolines. Atomistic simulations have also been made for other oil production chemicals including scale inhibitors<sup>2</sup> and dissolvers.<sup>3</sup> These studies have been focused on the interactions between the chemicals and their target surfaces, i.e., between scale-treating chemical and Barite or between corrosion inhibitors and mild steel surfaces. However, it is also necessary to consider the interaction of these oil field additives with the oil field reservoir rock and clay surfaces. Of particular interest at this time is the ability to tune the strength of the molecular sorption processes into the formation rock so as to increase the time period over which oil production additives are kept at the appropriate concentration in the oil. Abundant minerals in these rocks include clays and silicates. Clay minerals have recently been considered in this respect.<sup>4</sup> Quartz seems to be rather inert, and not likely to adsorb the inhibitors on its surface. In this study, we chose calcite, also an abundant mineral in oil reservoir rock formations, as a system capable of undergoing molecular sorption processes. As the first in a series of studies of corrosion inhibitor adsorption, we report force field parameters for calcite. The crystal morphology, surface energies, and hydration energies of calcite have been studied using atomistic simulation techniques.<sup>5-7</sup> However, all these simulations are based on static calculations, and may not be directly compared with the experimental results at nonzero temperatures. Ion polarization force fields for calcite<sup>8.9</sup> have been developed for the estimation of point defects and the thermal dependence of structural and elastic properties without regard for the interaction of clacite with organic molecules. Here, we report the enthalpy of immersion into various solvents with molecular dynamic (MD) simulations as a first application of the new force field. Results using molecular mechanics are also provided for comparison.

### 2. Force Field

We treat calcium carbonate (CaCO<sub>3</sub>) using standard valence terms (bond, angle, inversions) for the internal bonds of CO<sub>3</sub><sup>2-</sup> consistent with the way in which the solvent and organic molecules are represented. These valence parameters were optimized with the experimental infrared and Raman data on calcium carbonate. The charges for the carbonate ion were obtained from Quantum Mechanics (HF 6-31G\*\*) assuming a net charge of -2. The Ca charge was taken as +2. We used the standard Dreiding van der Waals parameters<sup>10</sup> for carbon and oxygen. We optimized the Calcium van der Waals parameters (assuming standard combination rules) so that the room-temperature density, cohesive energy and compressibility match experiment.

The potential energy is represented as

$$E = \sum_{\text{bonds}} E_{\text{s}} + \sum_{\text{angles}} E_{\text{a}} + \sum_{\text{inversions}} E_{\omega} + \sum_{\text{cross}} E_{\text{x}} + \sum_{vdW} E_{vdW} + \sum_{charges} E_{\text{coul}}$$
(1)

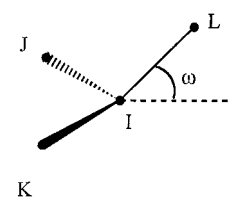
where the terms are defined below. The valence force field terms of carbonate were determined in such a way as to reproduce the experimental vibrational frequencies in the calcite crystal. The van der Waals parameters were optimized to reproduce the experimental cell parameters, density, and compressibility.

**2.1. Valence Parameters.** a. Harmonic Bond Stretch Term. Harmonic bond stretch term was represented by simple harmonic potential

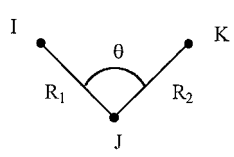
$$E_{\rm s} = \frac{1}{2} K_{\rm b} (R - R_0)^2 \tag{2}$$

<sup>\*</sup> To whom correspondence should be addressed † Present address: School of Chemistry, Seoul National University, Seoul 151-747, Korea

## **SCHEME 1. Inversion**



## **SCHEME 2. Cross Terms**



where  $R_0$  is the equilibrium bond distance in Å, and  $K_b$  is the force constant in kcal/(mol·Å<sup>2</sup>).

b. Harmonic Cosine Angle Bending Term. The angle bending term was in the form as follows

$$E_{\rm a} = \frac{1}{2}C(\cos\theta - \cos\theta_0)^2 \tag{3}$$

where  $\theta_0$  is the equilibrium angle and  $K_{\theta}$  is the force constant

$$K_{\theta} = C\sin^2\theta_0 \tag{4}$$

This form is preferred to the simple theta expansion because the cosine harmonic expansion satisfies the relations

$$E_{a}(\pi - \theta) = E_{a}(\pi + \theta) \tag{5}$$

and

$$E_{a}(-\theta) = E_{a}(\theta) \tag{6}$$

c. Inversion Term. The inversion term is of the umbrella type (spectroscopic force field) is as follows

$$E_{\omega} = K_{\omega} (1 - \cos \omega) \tag{7}$$

with a minimum for planar structure ( $\omega_0 = 0^{\circ}$ ),  $\omega$  is the angle between IL axis and the IJ K plane for an atom I with three bonds IJ, IK, and IL (See Scheme 1, inversion).

d. Bond-Angle and Bond-Bond Cross-Terms. To reproduce the vibrational frequencies correctly, we introduced the bondangle and bond-bond cross terms as follows

$$\begin{split} E &= D(R_1 - R_{1,0})(\cos\theta - \cos\theta_0) + E(R_2 - R_{2,0})(\cos\theta - \\ &\cos\theta_0) + K_{R_1R_2}(R_1 - R_{1,0})(R_2 - R_{2,0}) \end{split} \tag{8}$$

where the angle stretch force constants

$$K_{\theta,R_{\bullet}} = -D\sin\theta \tag{9}$$

and

$$K_{\theta,R_2} = -E\sin\theta \tag{10}$$

(See Scheme 2, cross terms).

**2.2. Nonbonded Interactions.** Nonbonded interactions are represented by electrostatic and van der Waals interactions. The van der Waals interactions have the exponential-six form

$$E_{\text{vdw}}(R) = Ae^{-CR} - BR^{-6} = D_0 \left\{ \left[ \left( \frac{6}{\zeta - 6} \right) \exp^{\zeta(1 - R/R_0)} \right] - \left[ \left( \frac{\zeta}{\zeta - 6} \right) \left( \frac{R_0}{R} \right)^6 \right] \right\}$$
(11)

and the standard combination rule  $(A_{ij} = (A_i \times A_j)^{1/2}, B_{ij} = (B_i \times B_j)^{1/2}, C_{ij} = 0.5 \times (C_i + C_j))$  is used.

The van der Waals parameters of carbon and oxygen atoms were taken from Dreiding II FF, <sup>10</sup> and those of calcium atom were optimized to reproduce the experimental cell parameters, density, and compressibility.

The electrostatic interactions are given by

$$E_{\text{coul}} = C_0 \frac{Q_i Q_j}{\epsilon R_{ii}} \tag{12}$$

where  $Q_i$  and  $Q_j$  are the atomic net charges (in electron unit),  $R_{ij}$  is the distance in Å,  $\epsilon$  is the dielectric constant ( $\epsilon = 1$  in present work), and the conversion factor  $C_0 = 332.0637$  takes care of the units, giving  $E_{\text{coul}}$  in kcal/mol.

The atomic net charges of oxygen and carbon were derived from the electrostatic potential fitting of carbonate ( $CO_3^{2-}$ ) at the level of HF/6-31G\*\*. Quantum mechanical calculation was performed with Jaguar v3.0 quantum chemistry software.<sup>11</sup> The charge of calcium ion was fixed at its formal charge of  $\pm 2|e|$ .

The van der Waals and electrostatic interaction were excluded for 1–2, and 1–3 interactions because they are considered to be already included in the bond stretch and angle bend terms. The nonbonding interactions are evaluated by the Ewald summation method<sup>12</sup> under full three-dimensional periodic bondary conditions.

## 3. Results and Discussion

- **3.1. Vibration Frequencies.** Because the force field of the carbonate was fitted to reproduce the experimental frequencies, the calculated frequencies are in excellent agreement with the experimental ones. <sup>13,14</sup> Note that vibrational frequencies from HF/6-31G\*\* on carbonate anion show 10–30 cm<sup>-1</sup> deviations even after the Poison-Boltzman solvation model <sup>15</sup> has been used to simulate the finite dielectric constant of the crystal.
- **3.2. Cell Parameters and Density.** Calcite has a rhombehedral crystal structure of spaces group  $R_{\bar{3}c}$  with six CaCO<sub>3</sub> in a unit cell. The calculated cell parameters and density are in excellent agreement with the experimental data.<sup>16</sup>
- **3.3. Compressibility.** The compressibility was calculated by two methods. The first method is the second derivative method, <sup>17</sup> which uses a single-point energy calculation to obtain the second derivatives of the lattice energy with respect to the lattice parameters and the atomic coordinates. The following energy expression is used

$$U = U_0 + \sum_{i} \frac{\partial U}{\partial \epsilon} \epsilon_i + \frac{1}{2} \sum_{ij} \frac{\partial U^2}{\partial \epsilon_i \partial \epsilon_j} \epsilon_i \epsilon_j + \text{higher order terms}$$
(13)

where  $U_0$  is equilibrium energy, and  $\epsilon$  is strain. When the structure is at an energy minimum, the second derivative term can be used to calculate the components  $C_{ij}$  of the stiffness matrix

$$C_{ij} = \frac{\partial U^2}{\partial \epsilon_i \partial \epsilon_j} \tag{14}$$

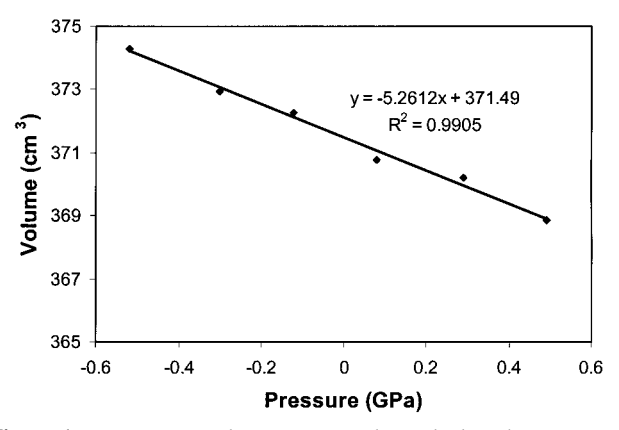


**Figure 1.** Pressure vs volume curve used to calculate the compressibility of calcite. Pressure and volume at each point are averaged over four 25 ps blocks from a 100 ps *NPT* MD sampling run after a 100 ps *NPT* equilibration run.

Then the adiabatic volume compressibility is calculated from the compliance matrix as follows

$$\beta = S_{11} + S_{22} + S_{33} + 2[S_{31} + S_{21} + S_{32}]$$
 (15)

where the compliance matrix, S, is the inverse of the stiffness matrix

$$\mathbf{S} = \mathbf{C}^{-1} \tag{16}$$

The compressibility calculated using the second derivative method is  $1.33 \times 10^{-2}~\text{GPa}^{1-}$  which is  $4{\sim}6\%$  smaller than the experimental values,  $1.38 \times 10^{-2} - 1.42 \times 10^{-2}~\text{GPa}^{1-}$ , at room temperature. The problem is that the energy minimization cannot account for the change in density with temperature and therefore should lead to a compressibility value lower than the room-temperature value.

To obtain the compressibility at room temperature, we use a second method based on the definition of volume compressibility

$$\beta = -\frac{1}{V_0} \left( \frac{\partial V}{\partial P} \right)_0 \tag{17}$$

In contrast to the previous static method, this compressibility is isothermal. The NPT dynamics were performed at various pressure, P=-0.5, -0.3, -0.1, 0.1, 0.3, and 0.5 GPa, and the compressibility was calculated from the slope of volume vs pressure curve. The temperature was maintained at 298.15 K by Nose–Hoover method. The pressure and volume values shown in Figure 1 were obtained from the averages of four 25 ps block averages of 100 ps MD runs after 100 ps equilibration runs. The value from MD simulation,  $1.42 \times 10^{-2}$  GPa<sup>1-</sup>, is in excellent agreement with experimental results.  $1.88 \times 10^{-2}$ 

**3.4. Lattice Energy.** The lattice energy of calcite can be defined as follows

$$\Delta H_{\rm L} = \Delta H_{\rm f}(\mathrm{Ca}^{2^{+}})(g) + \Delta H_{\rm f}(\mathrm{CO}_{3}^{2^{-}})(g) - \Delta H_{\rm f}(\mathrm{calcite})(c)$$
(18)

where  $\Delta H_{\rm L}$  is the lattice enthalpy,  $\Delta H_{\rm f}$  is the enthalpy of formation, and the symbols (g) and (c) represent the gas and crystal phases, respectively.  $\Delta H_{\rm L}$  represents the enthalpy release when the crystal is formed from its ions in the gas phase. The tabulated value of  $\Delta H_{\rm L}$  is 670 kcal/mol.<sup>24</sup> To estimate

TABLE 1: FF Parameters Used in Present Work

atom type descriptions					
Ca C_RC O_RC			calcium ion carbon in carbonate oxygen in carbonate		
bond stretching: $E_{IJ} = \frac{1}{2} K_b (R - R_0)^2$					
I	J	-	$K_{\rm b}({\rm kcal/(mol \mathring{A}^2)})$	R <sub>o</sub> (Å)	
C_RC	0_	RC	1134	1.2826	
angle bending: $E_{IJK} = \frac{1}{2} \frac{K_{\theta}}{\sin^2 \theta_0} (\cos \theta - \cos \theta_0)^2$					
I	J	K	$K_{\theta}$ (kcal/(mol rad <sup>2</sup> ))	$\theta_0(\deg)$	
O_RC	C_RC	O_RC	220.50	120	
	invo	maiam. F	$\pm V$ (1 - 2000)		

I	J	K	$K_{R_1\theta}$ (kcal/ (molÅrad))	$K_{R_2\theta}$ (kcal/ (molÅrad))	$K_{R_1R_2}$ (kcal/ (molÅ <sup>2</sup> ))
O_RC	C_RC	O_RC	102.00	102.00	211.0

Nonbonding: 
$$E(R) = D_0 \left\{ \left[ \left( \frac{6}{\zeta - 6} \right) \exp \zeta^{(1 - R/R_0)} \right] - \left[ \left( \frac{\zeta}{\zeta - 6} \right) \left( \frac{R_0}{R} \right)^6 \right] \right\} + 332.0637 \frac{Q_i Q_j}{R}$$

FF type	$R_{\rm o}({ m \AA})$	D <sub>o</sub> (kcal/mol)	ζ	$Q_{i}\left( \mathbf{e} \right)$
Ca	4.5500	0.6000	10.0000	+2.0000
C_RC	3.8963	0.0951	14.0340	+1.2046
O_RC	3.4046	0.0957	13.4830	-1.0682

 $\Delta H_{\rm L}$ , we calculated  $\Delta H_{\rm f}$  of each species by the following equation

$$\Delta H_{\rm f} = E_{\rm 0K} + ZPE + \Delta \Delta H_{0 \to 298 \, \rm K} \tag{19}$$

where  $E_{0~K}$  represents the energy at 0 K, ZPE is zero-point energy, and  $\Delta\Delta H_{0-298~K}$  is the enthalpy change from 0 K to room temperature.  $E_{0K}$  was obtained by energy minimization, the other terms were evaluated from the vibrational frequencies of the minimized structure of calcite for a 5 × 5 × 5 grid of points in the Brillouin zone using the PolyGraf modeling software. The result is  $\Delta H_{\rm f}$  ( ${\rm CO_3}^{2-}$ ) = 13.3 kcal/mol, and  $\Delta H_{\rm f}$  ( ${\rm Ca}^{2+}$ ) = 2.5 kcal/mol, and  $\Delta H_{\rm f}$  (calcite, one formula unit) = -681 kcal/mol. (See Table 2 for details.) This leads to  $\Delta H_{\rm L}$  = 697 kcal/mol, which is 4% higher than the  $\Delta H_{\rm L}$  value of 672 kcal/mol estimated in reference. Our evaluation of vibration frequencies through energy minimization uses cell parameters of calcite optimized at 0 K, which is likely to overestimate the lattice energy since the cell expands with temperature.

**3.5. Surface Energy.** To find the most stable surface for the subsequent adsorption studies, we cut the crystal to obtain five planar surfaces; (10.0), (00.1), (11.0), (10.1), and (10.4) surfaces.

TABLE 2: Results of the MM and MD Simulations

		encies

mode	exp (cm <sup>-1</sup> , calcite) <sup>a</sup>		$\frac{\text{HF/6-31G**}}{(\epsilon = 8)^c}$	$HF/6-31G** \ (\epsilon = 1)^d$	note
$\nu_1$	1085	1086	1063	1022	A <sub>1</sub> ', Raman sym. stretching
$\nu_2$	877	877	867	901	A2", IR out-of-plane
$\nu_3$	713	714	672	662	E', IR, Raman bending
$\nu_4$	1435	1438	1464	1450	E', IR, Raman asym. streching

	MM	MD (298.15 K)	exp
a (Å) c (Å) density (g/cm³) compressibility (1/GPa)	$4.999  16.975  2.714  1.331 × 10^{-2}$	$5.00_4 \pm 0.04$ $17.1_1 \pm 0.4$ $2.68_9 \pm 0.03$ $1.42 \times 10^{-2}$	$4.9896^e$ $17.061^e$ $2.706^e$ $1.38 \times 10^{-2}$ (ref 19) $(298.15 \text{ K})$ $1.39 \times 10^{-2}$ (ref 20) $(273.15 \text{ K})$ $1.40 \times 10^{-2}$ (ref 18) $(298.15 \text{ K})$ $1.41 \times 10^{-2}$ (ref 19) $(298.15 \text{ K})$ $1.42 \times 10^{-2}$ (ref 21)
lattice energy (kcal/mol)	697 <sup>f</sup>		(298.15 K) 672 <sup>g</sup> (298.15 K)

 $^a$  Raman active modes are taken from ref 14, and IR active modes from ref 13.  $^b$  from FF developed in the present work.  $^c$  from HF/6-31G\*\* calculation using Jaguar 4.0³¹ from HF/6-31G\*\* calculation with Poisson—Boltzmann solvation model ( $\epsilon=8$ , and  $r_{\rm probe}=1.94147$  Å) with scale factor of 0.8992.  $^d$  from HF/6-31G\*\* calculation using Jaguar 4.0²⁰ from HF/6-31G\*\* calculation with scale factor of 0.8992.  $^c$  Ref 16.  $^f$  This value is estimated by eq 19 and the following numerical values:  $E_{0~\rm K}$  (a calcite unit cell containing 6 CaCO<sub>3</sub>) =  $-4.192\times10^3$  kcal/mol, ZPE (a calcite unit cell containing 6 CaCO<sub>3</sub>) = 71.7 kcal/mol,  $\Delta\Delta H_{0-298~\rm K}$  (a calcite unit cell containing 6 CaCO<sub>3</sub>) = 33.5 kcal/mol,  $E_{0~\rm K}$  (carbonate) = 0.0 kcal/mol,  $E_{0~\rm$ 

Side views of these unit cells are shown in Figure 2, and surface energies are listed in Table 3. The unit cells for the surfaces comprised a three-layer-slab, and the surface energies were estimated by varying the unit cell lengths of the c-axis. The effect of surface relaxation was considered by relaxing all atoms (relaxation model 1), and comparing the results with the model in which no atom is relaxed (relaxation model 3), and the model in which the atoms in the central layer were fixed at their initial positions (relaxation model 2).

In all relaxation models, we find that the most stable surface is (10.4) surface, which agrees with previous calculations,<sup>5–7</sup> and with experimental observations.<sup>26,27</sup> There was little surface relaxation for this surface, which also indicates that this surface is quite stable. For (10.4), (10.0), and (11.0) surfaces, relaxation model 1 and 2 gave almost the same energy and atomic positions, indicating that the relaxation is localized at the surface boundary, as seen in Figure 3.

Using the bulk primitive unit cell for calcite (00.1) and (10.1) surfaces lead to dipolar surfaces with a net dipole perpendicular to the surface plane. This leads to a very slow convergence in the surface energy calculated as a function of the length of the c-axis. (See, for example, Figure 4 for (00.1) surface.) Thus, we modified the unit cell of the slab to remove the net dipole perpendicular to the surface. We did this by using a larger unit cell doubled over the original slab in a and/or b direction, and

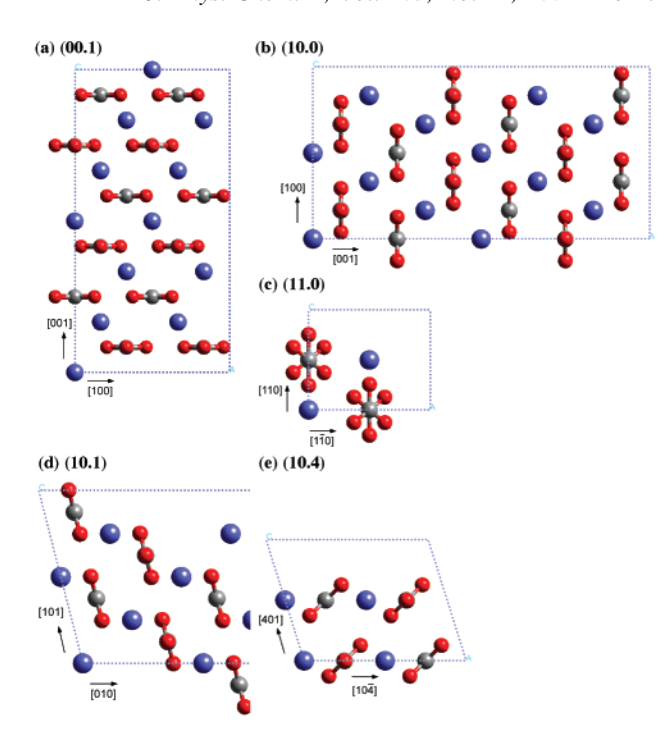


**Figure 2.** Side views of various calcite surfaces (unrelaxed). a) (00.1), (b) (10.0), (c) (11.0), (d) (10.1), and (e) (10.4) surfaces. Note that (10.4) surface is most stable, and that (00.1) and (10.1) surfaces are represented with doubled unit cell in a direction. This modification is for the removal of net dipole perpendicular to the slab.

TABLE 3: Calcite Surface Energies (unit: J/m²) from MM

surface	present work <sup>a</sup>	$\begin{array}{c} \text{present} \\ \text{work}^b \end{array}$	present work <sup>c</sup>	ref 5	ref 6	ref 7
(10.4)	0.93	0.86	0.86	0.23	0.60	0.59
(10.0)	3.12	1.37	1.37	0.52	1.59	0.97
$(00.1)^d(2 \times 2)$	2.69	1.45	1.44	1.60	$0.98^{e}$	$0.98^{e}$
$(00.1)^d(1 \times 2)$	2.68	1.45	1.44	1.60	$0.98^{e}$	$0.98^{e}$
$(00.1)^d(2 \times 1)$	2.68	1.45	1.44	1.60	$0.98^{e}$	$0.98^{e}$
$(10.1)^d(2 \times 2)$	2.38	1.49	1.49	N/A	$1.06^{e}$	$1.19^{e}$
$(10.1)^d(1 \times 2)$	2.38	1.49	1.49	N/A	$1.06^{e}$	$1.19^{e}$
$(10.1)^d(2 \times 1)$	3.09	1.42	1.42	N/A	$1.06^{e}$	$1.19^{e}$
(11.0)	2.05	1.66	1.66	0.50	1.43	1.39

<sup>a</sup> Without relaxation of atoms <sup>b</sup> With relaxation of atoms (central layer atoms are fixed) <sup>c</sup> With relaxation of atoms <sup>d</sup> Modified cell is used for the surface energy calculation <sup>e</sup> Averaged over two surfaces terminated in two different ways, either by a layer of calcium ions or by carbonate ions.

moving half of the surface ions of the extended unit cell to the other side of the slab. (See Figures 2, parts a and d.) The surface energies for three different extended unit cells are nearly identical to each other, as in Figure 4. The difference between the surface energy with fixed atom and that with relaxation, relaxation energy, was very large for these surfaces, as reported previously. Note that the surface energy of the present simulation is, in a sense, averaged over two different surface terminations because we used periodic boundary condition in three dimensions and calculated the energy with Ewald sums 12 in three dimensions.

The calculations using 5-layer-slab models gave the same quantitative results as obtained from 3-layer-slab models, which shows that 3-layer-slab model is suitable for the simulation.

**3.6. Enthalpy of Immersion.** The enthalpy of immersion of calcite in different solvents was reported in References.<sup>28,29</sup> The free energy of immersion is defined as

$$\Delta_{imm}G = \gamma_{sl} - \gamma_s \tag{20}$$

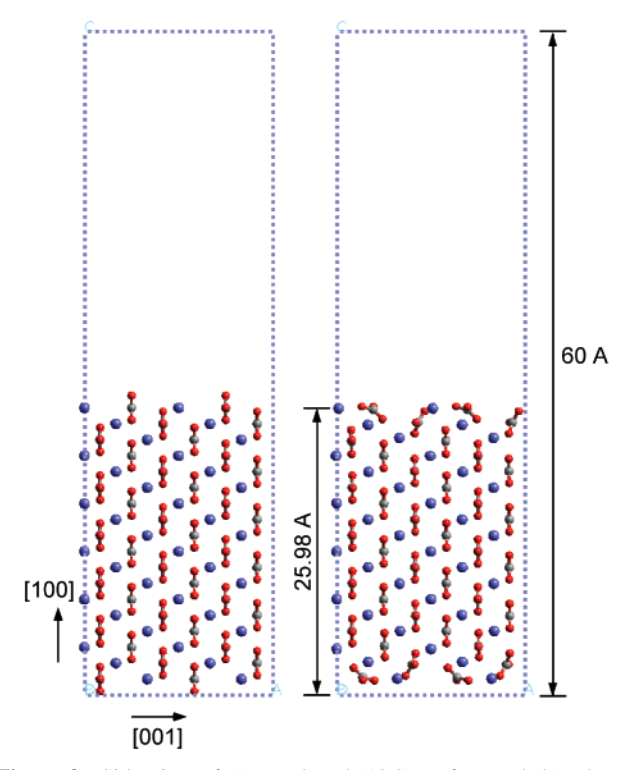


**Figure 3.** Side view of (a) unrelaxed (10.0) surface and (b) relaxed (10.0) surface. The relaxation is mainly localized at calcite/vacuum boundaries. The slab height is 25.98 Å for the 3-layer slab model, and the c-axis was extended to 60 Å in order to calculate the surface energy.

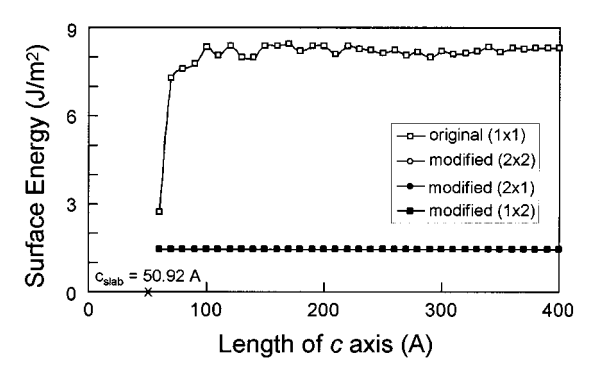


**Figure 4.** Surface energies of calcite (00.1) surface. Squares represents original (1  $\times$  1) in ab plane, and circles represent modified cell in (2  $\times$  2) in ab plane, filled circles represent (2  $\times$  1), and filled squares represent (1  $\times$  2) modifications. Note that surfaces energies for modified cells are nearly identical with each other, leading to 1.44 J/m². The slab height,  $C_{\rm slab}$  is 50.92 Å for 3-layer model of (00.1) surface.

where  $\gamma_{sl}$  is the surface tension of the solid—liquid (sl) interface and  $\gamma_s$  is the surface tension of the solid (s) in a vacuum. Then the enthalpy of immersion is described by the equation

$$\Delta_{imm}H = \Delta_{imm}G - T \left[ \frac{\partial (\Delta_{imm}G)}{T} \right]_{P}$$
 (21)

where T is the absolute temperature, and P is the pressure.

We calculated the enthalpy of immersion by molecular mechanics and molecular dynamics in the same way as in the surface energy calculation. The values of enthalpy of immersion were obtained by the difference between the calcite-solvent interface energy and surface energy of calcite

$$\Delta_{imm}H = \Delta \langle E \rangle_{\text{interface}} - \Delta \langle E \rangle_{\text{surface}}$$
 (22)

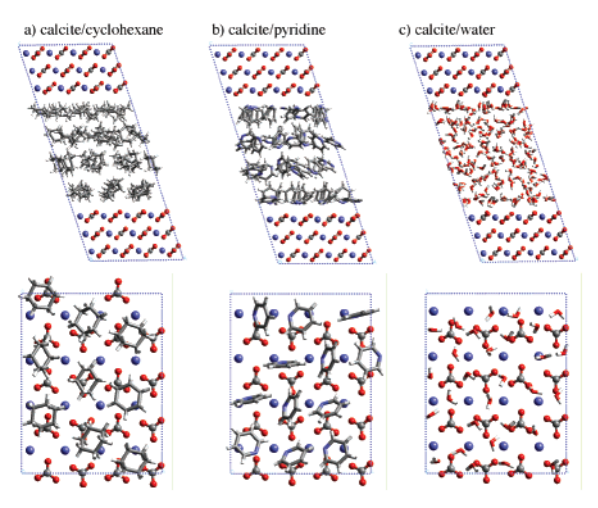


**Figure 5.** Side view (upper) and top view (lower) of the energy-minimized structure of the final snapshots from MD simulations: (a) calcite/cyclohexane b) calcite/pyridine, and (c) calcite/water.

where

$$\Delta \langle E \rangle_{\text{interface}} = \frac{\langle E \rangle_{\text{solid/solvent}} - \langle E \rangle_{\text{solid}} - \langle E \rangle_{\text{solvent}}}{2S} \quad (23)$$

and

$$\Delta \langle E \rangle_{\text{surface}} = \frac{\langle E \rangle_{\text{surface}} - \langle E \rangle_{\text{solid}}}{2S}$$
 (24)

Brackets signify the average over MD trajectories, and S is the surface area.

Among the various solvents experimentally measured, <sup>28,29</sup> we chose cyclohexane, pyridine, and water because these are representative of nonpolar, polar, and aqueous solvents, respectively. For cyclohexane, Dreiding II force field with exp-6 van der Waals parameter was used along with QEq charges. For pyridine, the Dreiding II force field with exp-6 van der Waals parameters was used along with charges obtained from ESP HF/6-31G\*\* calculation. For water, the F3C force field<sup>30</sup> was used. This force field is a flexible three-center water model.

The composite system containing both solvent and calcite was prepared from the following steps:

- 1. Building a solvent box using amorphous builder implemented in Cerius2 simulation package so that the density of solvent in the box reproduces the experimental bulk density, e.g.,  $0.7739 \text{ g/cm}^3$  for cyclohexane at room temperature. A  $\sim 20 \times \sim 20 \times \sim 20$  Å box for cyclohexane needs 45 molecules of cyclohexane. The length of the cell parameter is adjusted to satisfy the bulk density
- 2. Performing 10 ps NVT MD simulation of solvent box for cyclohexane, and 200 ps NVT runs for pyridine, and water. The length of the simulation time was chosen so that the 5 ps block average of the potential energy is converged within few kcal/mol.
- 3. Making a composite box by increasing the *c*-axis length of calcite solid resulting in a (10.4) surface slab, then by filling the space with the solvent molecules preequilibrated in step 2.
- 4. Performing a preliminary energy minimization with molecules in calcite fixed. This step is for the removing "bad" van der Waals contact at the solid/solvent interface.
- 5. Performing a full energy minimization with all atoms allowed to move.

**TABLE 4: Enthalpy of Immersion of Calcite in Different Solvents** 

ı	Cvc	اما	hexane	from	Λ	ÆΝ	/
1	CVC	LO.	nexane	пош	- 11	/111	/1

•		
quantities	values	units
E (calcite-cyclohexane)	-66381.0	kcal/mol
E (calcite)	-67067.3	kcal/mol
E (cyclohexane)	71.9	kcal/mol
interface energy <sup>a</sup>	0.664	$J/m^2$
surface energy <sup>b</sup>	0.863	$J/m^2$
energy of immersion <sup>c</sup>	-0.199	$J/m^2$
enthalpy of immersion (exp) <sup>d</sup>	-0.156	$J/m^2$

#### pyridine from MM

quantities	values	units
E (calcite/pyridine)	-73106.5	kcal/mol
E (calcite)	-67067.3	kcal/mol
E (pyridine)	-6518.1	kcal/mol
interface energy <sup>e</sup>	0.518	$J/m^2$
surface energy <sup>f</sup>	0.863	$J/m^2$
energy of immersiong	-0.345	$J/m^2$
enthalpy of immersion $(exp)^h$	-0.463	$J/m^2$

#### water from MM

quantities	values	units
E (calcite-water)	-69412.5	kcal/mol
E (calcite)	-67067.3	kcal/mol
E (water)	-2721.1	kcal/mol
interface energy <sup>i</sup>	0.406	$J/m^2$
surface energy <sup>j</sup>	0.863	$J/m^2$
energy of immersion <sup>k</sup>	-0.457	$J/m^2$
enthalpy of immersion (exp) <sup>l</sup>	-0.535	$J/m^2$

## cyclohexane from MD

MD results	average	stand. dev.	
PE (calcite/cyclohexane) (a)	-65410	2	kcal/mol
PE(calcite; bulk) (b)	-66640.1	0.4	kcal/mol
PE(cyclohexane) (c)	600	2	kcal/mol
interface Energy <sup><math>m</math></sup> {(a)-(b)-(c)}/	0.682	0.003	$J/m^2$
$(2 \times S)$ (d)			
PE(calcite; slab) (e)	-65833.7	0.4	kcal/mol
surface Energy <sup><math>n</math></sup> {(e)-(b)}/	0.872	$8 \times 10^{-6}$	$J/m^2$
$(2 \times S^o)$ (f)			
energy of immersion <sup><math>p</math></sup> (d)-(f) enthalpy of immersion (exp) <sup><math>a</math></sup>	-0.190 $-0.156$	0.0008	$J/m^2$ $J/m^2$

## pyridine from MD

MD results	average	std. dev.	
PE (calcite/pyridine) (a)'	-72222.98	5.93	kcal/mol
PE (pyridine) (c)'	-6073.85	1.85	kcal/mol
interface Energy' $\{(a)'-(b)-(c)'\}$	0.531	0.000	$J/m^2$
$(2 \times S^b)$ (d)'			
energy of immersion (d)'-(f)	-0.341	0.000	$J/m^2$
enthalpy of immersion <sup>t</sup> (exp)	-0.463		$J/m^2$

## water from MD

MD results	average	stand. dev.	
PE (calcite/water) (a)"	-68349.3	7.0	kcal/mol
PE (water) (c)"	-2067.2	2.8	kcal/mol
interface energy $\{(a)''-(b)-(c)''\}/$	0.387	0.005	$J/m^2$
$(2 \times S^w)$ (d)"			
energy of immersion <sup>x</sup> (d)"-(f)	-0.485	0.003	$J/m^2$
enthalpy of immersion (exp)	-0.535		$J/m^2$

<sup>a</sup> Eq 23. <sup>b</sup> Eq 24. <sup>c</sup> Eq 22. <sup>d</sup> Ref 28. <sup>e</sup> Eq 23. <sup>f</sup> Eq 24. <sup>g</sup> Eq 22. <sup>h</sup> Ref 29. <sup>i</sup> Eq 23. <sup>j</sup> Eq 24. <sup>k</sup> Eq 22. <sup>l</sup> Ref 28. <sup>m</sup> Eq 23. <sup>n</sup> Eq 24. <sup>o</sup> S = surface area. <sup>p</sup> Eq 22. <sup>q</sup> Ref 28. <sup>r</sup> Eq 23. <sup>s</sup> S = surface area. <sup>l</sup> Eq 22. <sup>u</sup> Ref 29. <sup>v</sup> Eq 23. <sup>w</sup> S = surface area. <sup>x</sup> Eq 22. <sup>y</sup> Ref 28.

6. Performing a 25 ps NVT MD simulation for calcite/cyclohexane box to obtain a converged potential energy. A 200 ps NVT run is performed for calcite/pyridine and calcite/water.

3.6.1. Calcite/Cyclohexane. For calcite/cyclohexane, we used 25 ps run of NVT dynamics with Hoover thermostat.<sup>23</sup> We took the first 10 ps as an equilibration period, and then three block averages of the potential energy over 5 ps each.

In Figure 5, we present the energy-minimized structures of final snapshots from the MD simulations, providing structural information on calcite immersed in solvents. Although randomly oriented in the bulk portion, the solvent molecules are aligned to maximize the interactions with the calcite surfaces at boundaries between solution and calcite layers. As seen in Figure 5a, the alignment is maintained roughly over a single layer. The orientation of the cyclohexane at the interfaces is random. Nine cyclohexane molecules form an interface layer at the solvent bottom, at which sixteen calcium carbonates are located. The random orientation indicates no specific interaction between cyclohexane and calcium carbonate exists.

3.6.2. Calcite/Pyridine. For calcite/pyridine, the equilibrium is rather slow, and thus, we performed a 200 ps run of NVT dynamics. The first 100 ps were taken as the equilibration period, and four block averages of the potential energy over 25 ps each.

For the calcite/pyridine system, the nitrogen atoms of pyridines are pointing to the calcite/pyridine interface and coordinated to the Ca<sup>2+</sup> ions (See Figure 5b). At the bottom interface, 12 pyridine molecules form an interface with the calcite. Nine molecules of these shows nitrogen atoms oriented toward Ca<sup>2+</sup> ions. This suggests that the adsorption of pyridine onto the calcite surface may lead to the wettability change from hydrophilic to hydrophobic found in the oil field rocks.<sup>29</sup>

3.6.3. Calcite/Water. As for pyridine, the equilibrium for water is also slow, and thus, we performed a 200 ps run of NVT dynamics. Like pyridine case, the first 100 ps were taken as the equilibration period, and four block averages of the potential energy over 25 ps each.

Water molecules are aligned so that hydrogen atoms are near the calcite surface, pointing to oxygen atoms in carbonate. (Figure 5c).

3.6.4. Discussion. The results for the enthalpy of immersion are reported in Table 4. The enthalpy of immersion into cyclohexane is 0.190 J/m² overestimated by 22%, whereas those into pyridine and water are 341 and 485 J/m², underestimated by 26% and 9%, respectively, when compared against experimental results. However, the experimental results may be subject to the adsorption of hydrophilic substances and surface defects. Simulations with the adsorption of organic molecules and water on the calcite surfaces are in progress and will be reported separately.

#### 4. Summary

As the first step in understanding the mechanism of corrosion inhibitor squeeze treatments, we developed force field parameters for calcite. The force field is optimized to reproduce the vibrational frequencies, cell parameters, density, and the compressibility of the calcite crystal. The force field reproduces the experimental stability of the calcite surfaces, and the heats of immersion into various solvents.

Acknowledgment. This research was initially funded by Saudi Aramco, continued under funding by Chevron Petroleum Technology Co., and completed under funding by the National Petroleum Office (NPTO) of the Department of Energy. Additional support for the facilities of the MSC was also provided by grants from DOE-ASCI, NSF (CHE 95-12279), BP Chemical, ARO-MURI, ARO-DURIP, the Beckman Insti-

tute, Exxon, Avery Dennison, 3M, Dow, General Motors, Kellogg, Seiko-Epson and Asahi Chemical. We thank Dr. Y. Tang for his helpful discussion.

## References and Notes

- (1) Ramachandran, S.; Tsai, B.-L.; Blanco, M.; Chen, H.; Tang, Y.; Goddard, W. A., III Langmuir 1996, 12, 6419.
- (2) Jang, Y. H.; Blanco, M.; Tang, Y.; Shuler, P.; Goddard, W. A., III. in preparation.
- (3) Blanco, M.; Tang, Y.; Shuler, P.; Goddard, W. A., III J. Mol. Engineer. 1997, 7, 491.
- (4) Hwang, S.; Blanco, M.; Demiralp, E.; Cagin, T.; Goddard, W. A., III J. Phys. Chem. B, 2001, 105, 4122-4127.
- (5) Parker, S. C.; Kelsey, E. T.; Oliver, P. M.; Titiloye, J. O. Faraday Discuss. 1993, 95, 75-84.
- (6) de Leeuw, N. H.; Parker, S. C. J. Chem. Soc., Faraday Trans. 1997, 93, 467-475.
- (7) de Leeuw, N. H.; Parker, S. C. J. Phys. Chem. B. 1998, 102, 2914-2922
- (8) Fisler D. K.; Gale J. D.; Cygan R. T. Am. Mineral. 2000, 85, 217-224.
- (9) Pavese, A.; Catti, M.; Parker S. C.; Wall A. Phys. Chem. Min. 1996, 23, 89-93.
- (10) Mayo, S. L.; Olafson, B. D.; Goddard, W. A., III J. Phys. Chem. 1990, 94, 8897.
  - (11) Jaguar v3.0; Schrodinger Inc.: Portland, Oregon, 1997
  - (12) Karasawa, N.; Goddard, W. A., III J. Phys. Chem. 1989, 93, 7320.
- (13) Coleyshaw, E. E.; Friffith, W. P.; Bowell, R. J. Spectrochim. Acta A **1994**, 50, 1909.

- (14) Anderson, F. A.; Brecevic Acta Chem. Scand. 1991, 45, 1018.
- (15) Tannor, D. J.; Marten, B.; Murphy, R.; Friesner, R. A.; Sitkoff, D.; Nicholls, A.; Ringnalda, M. N.; Goddard, W. A., III; Honig, B. A. J. Am. Chem. Soc. 1994, 116, 11 875-11 882.
- (16) Effenberger, H.; Mereiter, K.; Zemann, J. Z. Kristallogr. 1981, 156,
- (17) Cerius2 Property Prediction, April 1997.; Molecular Simulations Inc.: San Diego, 1997.
  - (18) Peselnick, L.; Robie, R. A. J. Appl. Phys. 1963, 34, 2494.
  - (19) Dandekar, D. P. J. Appl. Phys. 1968, 39, 2971-2973.
  - (20) Kaga, H. Phys. Rev. 1968, 172, 900-919.
- (21) Landolt-Boernstein Numerical Data and Functional Relationships in Science and Technology; Springer-Verlag: Berlin, 1979; Vol. 11.
  - (22) Nose, S. Mol. Phys. 1984, 52, 255-268.
  - (23) Hoover, W. G. Phys. Rev. A 1995, 31, 1695-1697.
- (24) Lide, D. R. CRC Handbook of Chemistry and Physics, 80 ed.; CRC Press: Boca Raton, 1999.
- (25) Polygraf v. 3.30; Molecular Simulations Inc.: San Diego, 1993. (26) Blanchard, D. L., Jr.; Baer, D. R. Surface Sci. 1992, 276, 27-
  - (27) Ohnesorge, F.; Binnig, G. Science 1993, 260, 1451-1456.
- (28) Lagerge, S.; Rousset, P.; Zoungrana, T.; Douillard, J. M.; Partyka, S. Colloids Surf., A. 1993, 80, 261-272.
- (29) Zoungrana, T.; Berrada, A.; Douillard, J.-M.; Partyka, S. Langmuir **1995**, 11, 1760-1767.
- (30) Levitt, M.; Hirshberg, M.; Sharon, R.; Laidig, K. E.; Daggett, V. J. Phys. Chem. B 1997, 101, 5051-5061.
  - (31) Jaguar v4.0; Schrodinger Inc.: Portland, Oregon, 2000.